

OMNIBAL: TOWARDS FAST INSTRUCT-TUNING FOR VISION-LANGUAGE MODELS VIA OMNIVERSE COMPUTATION BALANCE

Yongqiang Yao^{1,2*}, Jingru Tan^{3*}, Jiahao Hu², Feizhao Zhang²
Xin Jin², Bo Li⁴, Ruihao Gong^{2,5}, Pengfei Liu¹

{soundbupt}@gmail.com

¹Shanghai Jiao Tong University, ²SenseTime Research, ³Central South University

⁴Tongji University, ⁵Beihang University

ABSTRACT

Recently, vision-language instruct-tuning models have made significant progress due to their more comprehensive understanding of the world. In this work, we discovered that large-scale 3D parallel training on those models leads to an imbalanced computation load across different devices. The vision and language parts are inherently heterogeneous: their data distribution and model architecture differ significantly, which affects distributed training efficiency. We rebalanced the computational loads from data, model, and memory perspectives to address this issue, achieving more balanced computation across devices. These three components are not independent but are closely connected, forming an omniverse balanced training framework. Specifically, for the data, we grouped instances into new balanced mini-batches within and across devices. For the model, we employed a search-based method to achieve a more balanced partitioning. For memory optimization, we adaptively adjusted the re-computation strategy for each partition to utilize the available memory fully. We conducted extensive experiments to validate the effectiveness of our method. Compared with the open-source training code of InternVL-Chat, we significantly reduced GPU days, achieving about 1.8x speed-up. Our method’s efficacy and generalizability were further demonstrated across various models and datasets. Codes will be released at <https://github.com/ModelTC/OmniBal>.

1 INTRODUCTION

Developing large language models (LLM) has brought new possibilities to many fields. Multi-modal models, particularly Vision-Language Models (VLMs) Alayrac et al. (2022); Team et al. (2023a); Reid et al. (2024); Liu et al. (2023a); Bai et al. (2023b); Chen et al. (2023), are advancing rapidly due to their deeper understanding of the world. The training scale of VLM models is continually growing. More texts and images with higher resolution are used on the data level. Compared with the LLaVA-1.5 model Liu et al. (2023a), the InternVL-Chat Chen et al. (2024) model has expanded the dataset size from 665K to 5M and increased image resolution from 336x336 to 3840x2160. On the model level, larger vision encoders are adopted. The InternVL-Chat model upgrades the visual encoder from ~300M ViT-L-336px Radford et al. (2021) to ~6B InternViT-448px Chen et al. (2023). The scale of large models and datasets results in a time-consuming training process. Therefore, efficient training strategies are necessary for the field’s rapid development.

3D parallelism Shoeybi et al. (2019); Rajbhandari et al. (2020) is a popular framework for large-scale distributed training, which allows data and models to be distributed across multiple devices. Balancing computational load across devices is crucial in 3D parallelism, as it minimizes idle times and significantly improves training efficiency.

In this work, we found that for instruct-tuning large vision-language models, the heterogeneous nature of data and model structures brings new challenges to 3D parallelism training: (1) Varying

*Equal contribution with random order.

input sizes of texts and images cause fluctuating computational loads across training iterations and devices. (2) The heterogeneity of text and image encoders results in inherent differences in the computational load of their transformer blocks. Along with varying input sizes, this inevitably leads to uneven computational load and computational bubbles. (3) Input size variation and computational imbalance compel us to use the most aggressive re-computation (checkpointing) Li et al. (2014) strategy to prevent program crashes, which significantly wastes computational resources. We refer to those issues caused by the heterogeneity in data and model structures in large multi-modal models as the **Computation Imbalance** problem, which significantly reduces training efficiency.

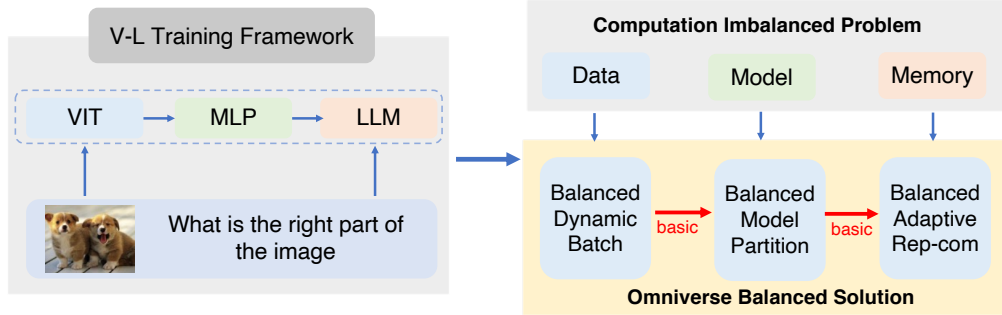


Figure 1: Left: Standard Vision-Language instruct-tuning framework. Right: Overview of the computation imbalanced problem and our proposed solution. We considered the bottleneck issues of data, model, and memory, and proposed an omniverse solution addressing these three aspects, with each providing the foundation for the next.

To address this problem, we propose a simple and efficient training framework called Omniverse Balance (**Omnibal**), to balance computational load across multiple devices. This framework systematically balances computation in three bottlenecks, *i.e.* data, model, and memory, as shown in Figure 1. Omnibal works in these three closely connected aspects. Data lays the groundwork for addressing model imbalances, while both data and model form the foundation for solving memory issues. Ultimately, these three aspects collaborate to achieve balanced computation. **Data:** We propose the balanced dynamic mini-batch method to group instances as new mini-batches according to text length and number of images. Specifically, an iterative algorithm based on sampling and filtering combines data of different sizes into balanced groups, ensuring consistent group sizes and stable input sizes; **Model:** We propose balanced model partitioning to evenly spread the computational loads of text and image models across devices. Using a search-based approach, this method efficiently finds optimal partition strategies within a small search space, enabling adaptation to different model architectures and hardware platforms. Our proposed balanced dynamic mini-batch method provides feasibility for balanced model partitioning by making input sizes consistent in advance. **Memory:** We propose the balanced adaptive re-computation to optimize the re-computation strategy on each device, maximizing memory utilization and training speed. We calculate the memory needs of various models to adjust the re-computation strategy adaptively. Notably, our proposed balanced dynamic mini-batch and model partitioning ensures balanced computational loads on each device, making memory analysis feasible.

We performed extensive experiments on various open-source VLM models at different scales, reducing overall training times significantly. We reduced GPU days for InternVL-Chat-1.5 (6+20B) from 61.8 to 21.3 GPU days under the Megatron-DeepSpeed microsoft (2020) backend. Scaling up to InternVL-Chat-1.5-Plus (6+34B), we consistently observed great speed-up, from 75.4 to 30.5 GPU days. We have conducted thorough generalization experiments, including various datasets, hardware configurations, and multiple model combinations. Consistent and significant improvements were observed across all experiments, demonstrating the effectiveness and versatility of our approach.

2 RELATED WORK

2.1 LARGE LANGUAGE MODEL (LLM)

Large language models, such as ChatGPT OpenAI (2023a), GPT-4 OpenAI (2023b), Llama series Touvron et al. (2023a;b); AI (2024), and Gemini series Team et al. (2023b); Reid et al. (2024), have seen significant advancements recently. These models leverage vast amounts of data to perform self-supervised learning by predicting the next token in a sequence. Large language models have demonstrated powerful generalization capabilities across various tasks, particularly in few-shot and zero-shot scenarios. Following the scaling law, the performance of these models improves with increases in model and data scale. Researchers have observed that LLMs exhibit emergent phenomena when the training scale reaches a certain threshold, showing sudden improvements in language understanding capabilities. Therefore, existing large language models are often trained at super large scales.

2.2 MULTI-MODAL LARGE LANGUAGE MODEL (MLLM)

Although LLM can be applied to various NLP tasks, they are typically built on textual data and can only accept text inputs. However, real-world scenarios often involve rich multi-modal information, typically images. It has driven the development of large vision language models (VLMs). Visual encoders like Vision Transformer (ViT) Dosovitskiy et al. (2021) are usually used to incorporate vision information. A cross-modal connector is also required to align the vision encoder outputs to the language models. LLaVA Touvron et al. (2023a) use the simplest MLP, BLIP series Li et al. (2022; 2023); Dai et al. (2024) use Q-former, Qwen-VL-Chat Bai et al. (2023b) use a cross-attention module. VLMs significantly expand large models' capabilities and application scenarios by instruct-tuning with text and image data. However, introducing multi-modal data and heterogeneous encoders also brings new challenges to the model training process.

2.3 LARGE-SCALE DISTRIBUTED TRAINING

Distributed training is essential for efficiently utilizing multiple GPUs to train large language models. It is achieved through 3D parallelism Shoenberger et al. (2019); Rajbhandari et al. (2020): data, tensor, and pipeline parallelism. *Data Parallelism* splits the entire dataset into mini-batches and assigns them to multiple devices, each with a model replica. This approach maximizes the use of GPU power for large datasets. DeepSpeed Zero Rajbhandari et al. (2020) enhances it by reducing weight redundancy. However, it can still be challenged by the memory limits of individual devices when handling huge models. *Tensor Parallelism* distributes a model's weight matrices across multiple devices, enabling parallel matrix operations Shoenberger et al. (2019) and reducing per-device memory requirements. This method accelerates computation but requires dense inter-device communication, typically restricted to single-node deployments to minimize latency. *Pipeline Parallelism* divides a deep learning model into segments and assigns them to different devices, creating a computation flow like a production line. This technique facilitates larger model scaling across nodes. GPipe Huang et al. (2019) proposes micro-batching. PipeDream Narayanan et al. (2019) further proposes a one-forward-one-backward (1F1B) scheme to optimize memory usage. In pipeline parallelism, uneven layer partitioning can cause significant pipeline bubbles. DreamPipe Narayanan et al. (2019) and AdaPipe Sun et al. (2024) optimize model partitioning and re-computation strategies based on profiling and dynamic programming, respectively. However, these advancements are primarily tested in text-based models and may require adaptation for large multi-modal scenarios.

3 COMPUTATION IMBALANCE

In this section, we explore the unique challenges of large-scale distributed training for vision-language models, focusing on three key aspects: data, model, and memory.

Data Imbalance: LLMs are trained on pure text data using next-token prediction as the objective. This allows arbitrary extraction of text sub-strings for batch training, ensuring consistent input lengths. In contrast, VLMs are trained on texts and images, requiring data integrity to be maintained without arbitrary truncation. The varying number of images, their resolutions, and text lengths in

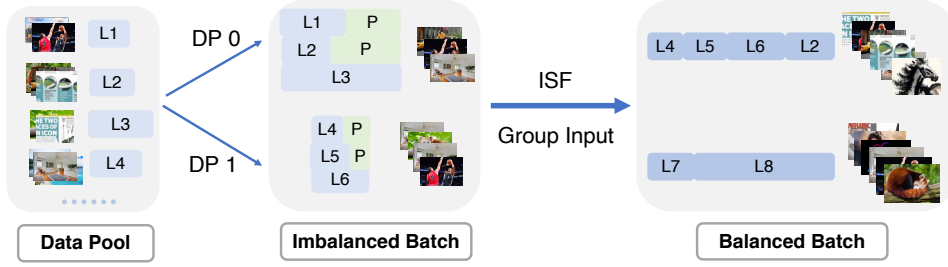


Figure 2: Left: Conventional mini-batch construction method. It has a severe imbalance problem, including within-device (excessive padding) and cross-device (varying data sizes) aspects. Right: Our proposed ISF is to build balanced mini-batches dynamically.

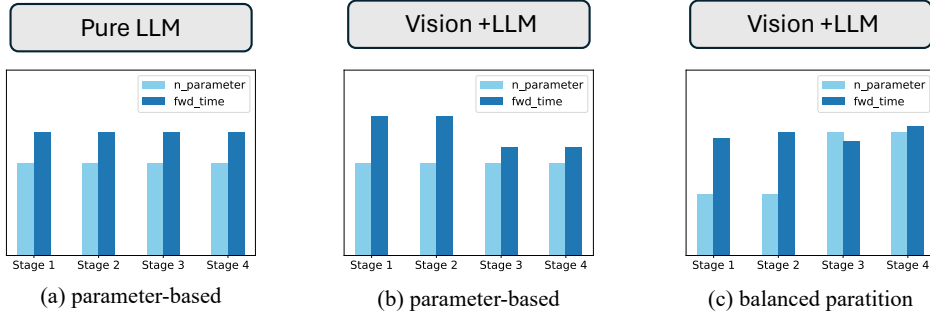


Figure 3: Illustration of the model imbalance problem. (a) In pure LLM, a balanced parameter partition cross devices (stages) means balanced computation time. (b) In LLM+Vision, a balanced parameter partition may result in significant computation time differences. (c) Our method achieves more balanced computation time, taking into account the characteristics of the language and the vision model.

different samples lead to significantly different input sizes between mini-batches (see Figure 2 left part). We can see that when combining individual training samples into a mini-batch, the input sizes on different data-parallel ranks *i.e.* DP0 and DP1 vary significantly. This variation leads to imbalanced computational loads among devices compared to pure LLM training, increasing GPU idle time. Furthermore, input size variations impact the model and memory.

Model Imbalance: LLMs use identical transformer modules with the same computational loads. Evenly dividing these layers in pipeline parallelism distributes the load effectively. However, VLMs require additional image pre-processing, necessitating an image encoder like ViT-L Dosovitskiy et al. (2021) before using text encoders like Llama Touvron et al. (2023a). Structural differences between image and text encoders result in varying computational demands. For example, for the InternVL-Chat-1.5 structure Chen et al. (2024), the image encoder has 45 layers and 6B parameters, and the text encoder has 48 layers and 20B parameters. When using 9 images and 4K text input, the image encoder’s computation time can account for almost 40% of the total. As a result, partitioning the model based on layers or parameters can lead to imbalanced loads and increased pipeline bubbles, as shown in Figure 3. More importantly, varying text and image input sizes in VLM training make it difficult to estimate the computational demands of image and text encoders precisely, further complicating model partitioning.

Memory Imbalance: LLMs require significant GPU memory due to their large parameter size. When memory is insufficient, re-computation Li et al. (2014) techniques discard some intermediate activation values and recompute them during backward propagation to save memory. VLM encounters significant memory challenges due to the variable scales of data inputs and the heterogeneity between vision and language models. Sometimes, many images or long texts that appear occasionally can demand excessive GPU memory, so we have to use the most aggressive re-computation

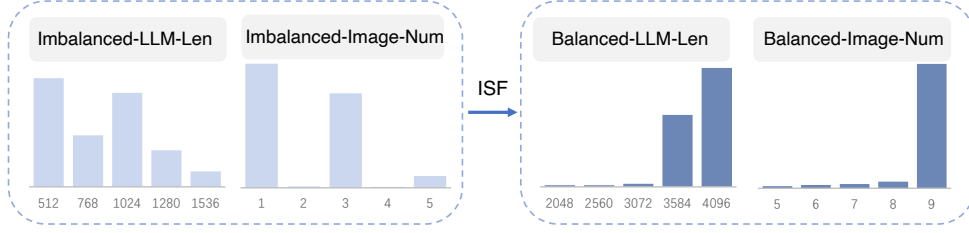


Figure 4: Illustration of imbalanced data problem in both language and vision part. The ISF makes the data distribution more concentrated.

configuration to prevent the program from crashing. However, excessive re-computation can significantly slow down the training process.

4 METHOD

This section presents our computation-balanced framework OmniBal for training large vision-language models. To address imbalanced computational loads across devices, we first manage the large variations in data input sizes, which is the most fundamental issue in the computation imbalance problem. This enables the possibility of balanced model partitioning. Finally, we optimize the re-computation strategy for each partition.

4.1 BALANCED DYNAMIC MINI-BATCH

Due to the inherently paired nature of the data used for training VL models, each sample contains various images and text segments, resulting in non-fixed input sizes. We evaluated input imbalance from two perspectives: within-device samples and cross-device mini-batches.

Pad ratio (within-device): When combining samples of different sizes into a mini-batch, smaller samples need to be padded to ensure uniform input sizes. The pad ratio is calculated as follows:

$$PadRatio = \frac{\sum_i^N (nt_{max} - nt_i)}{nt_{max} \times B} \quad (1)$$

Where nt_{max} represents the maximum number of tokens in a mini-batch of size B , and nt_i denotes the number of tokens for sample i within that mini-batch.

Dist ratio (cross-device): Even after padding, the sizes of mini-batches on different devices may vary, leading to different input scales across devices. The distribution ratio is calculated as follows:

$$DistRatio = \frac{\sum_i^{ND} (NT_{max} - NT_i)}{NT_{max} \times ND} \quad (2)$$

Where ND represents the number of devices, NT_{max} denotes the maximum number of mini-batch tokens across all devices, and NT_i refers to the number of mini-batch tokens on the i^{th} device. Non-fixed input sizes in VLMs have a larger pad ratio and dist ratio, as shown in Table 4 (row 1). A high pad ratio wastes computational resources, while a high dist ratio causes device idle time. They significantly impact training throughput efficiency.

To address this issue, we adaptively group multiple samples to ensure that the new samples have image and text sizes within a relatively fixed range, which we refer to as a Balanced Dynamic Mini-Batch, as illustrated in Figure 2. However, determining the optimal grouping strategy is a challenging problem. We have designed an iterative method using sampling and filtering to select an optimal grouping strategy. As illustrated in Algorithm 1 and Algorithm 2, our method **Iterative Sampling and Filtering (ISF)** involves the following steps:

Algorithm 1 ISF: Sampling Stage

```

1:  $\mathcal{D} = \text{randperm}(\mathcal{D})$ , set  $\mathcal{G} = [ ]$ 
2: for  $(x_i, y_i)$  in  $\mathcal{D}$  do
3:    $\mathcal{G} \leftarrow \mathcal{G} + (x_i, y_i)$ 
4:   if  $I_v > Q_v$  or  $I_t > Q_t$  then
5:      $\mathcal{G} \leftarrow \mathcal{G} - (x_i, y_i)$ 
6:      $\mathcal{P} \leftarrow \mathcal{P} + \mathcal{G}$ , set  $\mathcal{G} = [(x_i, y_i), ]$ 
7:   end if
8: end for
9: return  $\mathcal{P}$ 

```

Algorithm 2 ISF: Filtering Stage

```

1: Get  $\mathcal{P}$  from Sampling Stage
2: for  $\mathcal{G}$  in  $\mathcal{P}$  do
3:   if  $I_v < Q'_v$  and  $I_t < Q'_t$  then
4:      $\mathcal{P} \leftarrow \mathcal{P} - \mathcal{G}$ 
5:   else
6:     remove all  $(x_i, y_i)$  of  $\mathcal{G}$  from  $\mathcal{D}$ 
7:   end if
8: end for
9: return  $\mathcal{P}, \mathcal{D}$ 

```

1. Sampling Stage: For current dataset $\mathcal{D} = \{(x_i, y_i) \mid i\}$, we randomly add samples d_i consisted of images x_i , text y_i to current group \mathcal{G} . If the total number of images $I_v = \sum_{x_i \in \mathcal{G}} |x_i|$ or the total text length $I_t = \sum_{y_i \in \mathcal{G}} |y_i|$ reaches the predefined maximum number of images Q_v or text Q_t , we add this group to the candidate set \mathcal{P} and create a new group containing (x_i, y_i) for the subsequent samples. Otherwise, we will continue adding samples to the current group. At the end of the sampling stage, we will have a candidate set $\mathcal{P} = \{\mathcal{G}_i \mid i = 1, 2, 3, \dots\}$.

2. Filtering Stage: We first define the target number of images Q'_v and text Q'_t . For each group \mathcal{G}_i in candidate set \mathcal{P} , we filter \mathcal{G} whose image number I_v or text length I_t do not satisfy $I_v \geq Q'_v$ or $I_t \geq Q'_t$. We update the dataset \mathcal{D} by removing all satisfying samples (x_i, y_i) of the filtered group \mathcal{G}_i in \mathcal{P} from \mathcal{D} , and removing all non-satisfying samples within \mathcal{P} . Ultimately, \mathcal{P} becomes our final target set.

We repeat the sampling and filtering stages alternately for a maximum of T times. We acquire the candidate set \mathcal{P} each time, which includes more valid sample groups \mathcal{G} . Meanwhile, we have the updated dataset \mathcal{D} consisting of unselected samples, which is used for sampling and filtering in the next iteration. To ensure that the mini-batches constructed by the ISF method achieve lower pad ratio and dist ratio, we need to determine appropriate values for Q_v or text Q_t . The optimal values for Q_v or text Q_t vary across different datasets. In practice, we use a statistical approach described in Section 5.1 to determine these values. As shown in Figure 4, we can see that with ISF, the data distribution becomes more concentrated, indicating more balanced input sizes.

4.2 BALANCED MODEL PARTITIONING

With the input data sizes fixed, we carefully divide the model parameters across devices. Given the number of layers L in the model and the pipeline parallel size N , our goal is to find an optimal partition strategy $P = (P^{(1)}, P^{(2)}, P^{(3)}, \dots, P^{(N-1)})$ such that the training speed of the model is maximized. Here, $P^{(1)} < P^{(2)} < P^{(3)} < \dots < P^{(N-1)}$, and the i^{th} partition M_i consists of layers L_k , where $P^{(i-1)} \leq L_k < P^{(i)}$, with $P^{(0)} = 1$ and $P^{(N)} = L + 1$. For example, given a model with $L = 20$ layers and pipeline size $N = 4$, assume that we have an optimal partition $P = (5, 10, 15)$. The first partition M_1 consists of layers L_1, L_2, \dots, L_4 since $P^{(0)} = 1, P^{(1)} = 5$.

However, achieving balanced pipeline partitioning for VLMs is a more challenging task compared to LLMs. We must consider: (1) *Model Heterogeneity*: The structural differences between visual and language models make simple parameter-based or layer-based partition strategies unsuitable. (2) *Communication Overheads*: Different partition strategies have different communication volumes since the activation number of each layer may vary significantly in VLMs. (3) *Hardware Variability*: Different platforms have varying capabilities. Some platforms could have negligible communication overhead due to high network bandwidth. We designed a heuristic search algorithm based on the above analysis to find the optimal partition. We first identified a set of partitions that possibly contain the optimal solution $\{P_k = (P_k^{(1)}, P_k^{(2)}, P_k^{(3)}, \dots, P_k^{(N-1)}) \mid k = 1, 2, 3, \dots\}$. Then, we select the optimal partition P^* based on actual running time:

$$P^* = \arg \min_{P_i} f(P_i) \quad (3)$$

Here, $f(P_i)$ is the average running time obtained from training the model for 20 iterations under partition $f(P_i)$.

Partition Candidates: We start by profiling each layer’s computation time $\text{FWD}(L_i)$. A greedy algorithm is employed to compute the anchor partition P^+ , where the computation time of sub-model M_i is close. Around anchor partition P^+ , we create a set of partition candidates by jittering $P^{(1)}, P^{(2)}, P^{(3)}, \dots$ within a radius of r layers. There are total $3 \times 3 \times 3 = 27$ partition candidates when $r = 1, N = 4$.

Partition Metrics: When r and N are very large, there will be a significant number of partition candidates, making it inefficient to run and evaluate the time for each one. Therefore, we designed two metrics to rank these candidates.

The first metric is the difference in running time between different pipeline stages. Smaller differences generally result in fewer bubbles and, therefore, faster execution. We use the variance of the running times of different pipeline stages to measure this difference.

$$\text{VAR}(\text{fwd_time}) = \sum_{i=1}^N (\text{FWD}(M_i) - \overline{\text{FWD}(M_i)})^2 \quad (4)$$

The second metric is the total point-to-point communication volume of the partition strategy P_i . It depends on P_i consisting of $(P^{(1)}, P^{(2)}, P^{(3)}, \dots)$

$$\text{SUM}(\text{comm}) = \sum_{i=1}^{N-1} \text{ACTIV}(L_{pi}) \quad (5)$$

Where L_{pi} is the last layer of partition strategy $P^{(i)}$ and $\text{ACTIV}(L_{pi})$ is the activation number of layer L_{pi} , indicating the point-to-point communication of this partition strategy $P^{(i)}$. We use the sum of $\text{VAR}(\text{fwd_time})$ and $\text{SUM}(\text{comm})$ as the metric for the partition and rank them to select the top K candidates for speed evaluation.

4.3 BALANCED ADAPTIVE RE-COMPUTATION

Thanks to our proposed balanced dynamic mini-batch and balanced model partition, we have balanced computational loads for each partition. The memory requirements are also fixed because the computational demand has been fixed. Therefore, we can adjust the optimal re-computation strategy based on memory needs instead of using the most aggressive strategy to prevent crashes. Fewer re-computations accelerate the model’s backward step, significantly improving the training speed.

Additionally, we found that heterogeneous architectures have different memory requirements. For example, the vision model in InternVL-Chat-1.5 requires more GPU memory than the language model under the same computational load. Therefore, we need to individually analyze the memory requirements for each layer of vision and language models and adaptively set the optimal re-computation strategy for each layer. Specifically, we first calculate the memory required for each layer of vision or language models through profiling. Next, according to the remaining memory of each device, we determine the number of layers in a sub-model M_i where the re-computation strategy can be canceled.

5 EXPERIMENTS

In this section, we first introduce the models and datasets. Then, we demonstrate the acceleration achieved compared to current state-of-the-art VL models. Following that, we provide a detailed comparison of each component proposed in our method and its contribution to training acceleration. Finally, we conduct extensive experimental analysis.

Table 1: Main Results. We use open-source InternVL-Chat-1.5 6+20B and 6+34B as the models with either DeepSpeed (ZeRO-3) or Megatron-Deepspeed backend. We report GPUS Days in the InternVL-Chat-1.2 1.2M training dataset to show the speed-up ratio. Models are also evaluated on five commonly used benchmarks.

Model	Balance?	Backend	MMB-EN/CN	ChartQA	AI2D	MMVet	MME	GPU Days (speed-up)
6+20B	×	DeepSpeed	78.2/77.4	86.2	71.3	48.9	1901.2	38.9 (1x)
	✓	DeepSpeed	78.7/77.6	86.5	71.4	50	1969.4	25.3 (1.54x)
	×	Megatron	79.5/77.7	87.3	71.6	45.0	1957.7	61.8 (0.63x)
	✓	Megatron	78.6/77.5	86.7	70.9	48.5	1956.3	21.3 (1.83x)
6+34B	×	DeepSpeed	80.0/79.2	86.6	73.4	45.9	2015.8	54.3 (1x)
	✓	DeepSpeed	80.9/79.0	89.1	73.3	47.0	2153.6	35.5 (1.53x)
	×	Megatron	80.2/79.3	88.9	73.7	44.2	2111.9	75.4 (0.72x)
	✓	Megatron	80.1/78.0	89.3	73.5	45.4	2072.7	30.5 (1.8x)

5.1 EXPERIMENTAL SETUP

Model & Dataset setting: We conduct experiments following the open-source InternVL-Chat-1.5 setting. Our vision and language models are InternViT-6B and InternLM2-20B, respectively. We employ two configurations: InternVL-Chat-1.5 (6+20B) and InternVL-Chat-1.5-Plus (6+34B). As the InternVL-Chat-1.5 dataset is not yet available, we utilize the InternVL-Chat-1.2 dataset, which comprises approximately 1.2 million samples, as an alternative. All other training settings remain unchanged. We use GPU Days as our evaluation metric to estimate the total computing time. Specifically, we report GPU Days based on A100 GPU usage to evaluate the speed-up performance.

Implementation Details: We determine Q_v or text Q_t by using use statistics of datasets. First, we traverse the entire dataset and collect the summation of the lengths of all text tokens and the number of images. Then, We calculate the average number of text tokens per image. We set $Q_t = 4K$ as the length of the longest text token in the dataset and use the calculated text-to-image ratio to determine $Q_v = 9$. For images, we set $Q'_v = Q_v$, and for text, we set $Q'_t = Q_t - 128$.

5.2 MAIN RESULTS

We demonstrate the superiority of our method under various settings in Table 1. Our baseline model is InternVL-Chat-1.5 (6+20B) Chen et al. (2024), and we follow their setting, using DeepSpeed ZeRO-3 as the training backend. Our proposed method reduced GPU days from 38.9 to 25.3, achieving a 1.54x speedup. Simultaneously, we consistently maintained comparable performance across commonly used datasets, such as MMB-EN/CN Liu et al. (2023c), ChartQA Masry et al. (2022), AI2D Kembhavi et al. (2016), MMVet Yu et al. (2023), and MME Fu et al. (2023).

We conducted experiments using another advanced training framework, Megatron-DeepSpeed. Unlike DeepSpeed, Megatron-DeepSpeed integrates tensor and pipeline parallelism alongside data parallelism, enhancing its suitability for larger-scale models. However, directly applying 3D parallelism can slow down training due to the heterogeneous nature of VLM models, which complicates balanced partitioning and leads to computational inefficiencies. The table shows that switching to Megatron-DeepSpeed increased GPU days from 38.9 to 61.8. Our method addresses this issue by achieving computational balance across data, model, and memory. Utilizing our approach, we significantly reduced GPU days from 61.8 to 21.3, demonstrating that computational balance is crucial for effective 3D parallelism. Notably, our method also outperformed DeepSpeed, reducing GPU days from 25.3 to 21.3, highlighting the superiority of 3D parallelism when balanced computation is achieved.

We also report results under a larger-scale setting (InternVL-Chat-1.5-Plus) to verify the generalizability of our method. The larger model consistently improved, accelerating the training process while maintaining model performance. Specifically, we achieved speedups of 1.53x with the DeepSpeed backend and 1.8x with the Megatron-DeepSpeed backend.

Table 2: Training time of different settings

data balance	model balance	memory balance	GPU Days
			61.8
✓			51.9
✓	✓		29.0
✓	✓	✓	21.3

Table 3: Results on different datasets

Dataset	Dist Ratio		GPU Days
	<i>VIT</i>	<i>LLM</i>	
LLava-665K	0.02	0.145	43.3→12.4
InternVL-1.2M	0.02	0.14	61.8→21.3
LCS-558K	0.001	0.029	23.8→7.5

Table 4: Importance of data balance. AVE-BS indicates the average batch size in each iteration. We report results with Model Balance (MB) and without MB.

Method	AVE-BS	Max-Seq-Len		Pad Ratio	Dist Ratio		Balanced	GPU Days	
		<i>VIT</i>	<i>LLM</i>		<i>VIT</i>	<i>LLM</i>		w/o MB	w MB
baseline	4	20K	16K	0.31	0.34	0.30	×	61.8	42.2
sorted	4	20K	16K	0.014	0.47	0.40	×	54.0	40.0
device-group	4	20K	16K	0.378	0.125	0.228	×	54.5	43.6
ISF(ours)	4.6	9K	4K	0	0.02	0.14	✓	51.9	29.0

5.3 ABLATION ANALYSIS

In this section, we conduct ablation experiments on each component of our method, using InternVL-Chat-1.5 as the baseline model with a 3D parallel Megatron-DeepSpeed backend. Table 2 illustrates the impact of each part of our method. Due to computational imbalance, the baseline model’s training speed is very slow, requiring 61.8 GPU days. By achieving data balance, GPU days are reduced from 61.8 to 51.9. This improvement enables us to achieve a more balanced model partition, further reducing the training time to 29 GPU days. Finally, optimizing memory usage with an adaptive re-computation strategy reduces GPU days from 29.0 to 21.3. These results demonstrate that a holistic balance encompassing data, model, and memory is crucial for ensuring efficient training speed in VLM training. Below, we provide a more detailed analysis of each component.

The Importance of Data Balance: In Table 4, we investigate the importance of maintaining data balance in large-scale distributed training. We compared four methods: (1) Baseline Method: Randomly combining data into a mini-batch and padding according to the longest input in the mini-batch. (2) Sorted Method: Combining samples with similar text and image sizes into a mini-batch to minimize padding within devices. (3) Device-group Method: Grouping samples with similar text and image sizes across devices to minimize idle times. (4) Our Balanced Dynamic Mini-batch Method: Using Iterative Sampling and Filtering (ISF) to combine mini-batches dynamically. This comparison highlights the effectiveness of our Balanced Dynamic Mini-batch method in achieving superior data balance and optimizing training efficiency.

From the table, we can observe the following: (1) Baseline Approach: The baseline approach is the slowest due to the completely random combination of different-sized samples, which causes significant size variation within a mini-batch. This leads to excessive padding, with a padding ratio of 0.31. Additionally, there is considerable variation in mini-batch sizes across different devices, as evidenced by the Dist Ratio of 0.34 for ViT and 0.30 for LLM. This results in significant computation disparities between devices, causing many devices to idle and wait, thereby severely impacting the model’s throughput efficiency. (2) Sorted Method: This method enhances throughput efficiency by pre-grouping samples of similar sizes into mini-batches, thus reducing the internal padding ratio to 0.014. Minimizing the number of redundant tokens within mini-batches effectively lowers the GPU days required to 54.0. (3) Device-Group Method: This method aims to reduce device idle time by ensuring consistent input sizes across devices. It significantly improves the Dist Ratio for ViT and LLM, reducing them to 0.125 and 0.228, respectively. However, this approach only balances input sizes between devices and neglects the balance within mini-batches on each device. As a result, excessive padding occurs, with a padding ratio of 0.378, wasting substantial computational resources. (4) Our Approach: Our approach balances input sizes within mini-batches on each device and across devices simultaneously. As shown in the table, it reduces both padding and the Dist

Table 5: Importance of model balance. VAR indicates variance. SUM(comm) is the summation of commutation volume (MByte)

Method	VAR(param)	VAR(num.layer)	VAR(fwd.time)	Δ SUM(comm)	GPU days
(1) parameter-based	0.03	<u>13.4</u>	93.6	+0.0	42.2
(2) layer-based	<u>0.64</u>	1.2	20.1	+8.2	30.6
(3) profile-based	0.85	2.1	6.5	+16.6	30.9
(4) BMP (ours)	0.83	1.5	<u>12.2</u>	-21.0	29.0

Table 6: Importance of memory balance. VRAM_i denotes remaining VRAM(G) in parallel stage i . For the baseline model, the metric varies as minimum \sim maximum.

Method	V-Seq-Len	L-Seq-Len	VRAM_1	VRAM_2	VRAM_3	VRAM_4	GPU Days
baseline	4K \sim 20K	1K \sim 16K	13 \sim 50.2	7.3 \sim 40.5	7.3 \sim 40.5	7.3 \sim 40.5	61.8
+ data & model balance	9K	4K	58.2	56.2	32.5	32.7	29.0
+ memory balance	9K	4K	12.3	21.7	24.7	30.0	21.3

Ratio, achieving a padding ratio of 0 while maintaining very low Dist Ratios of 0.02 and 0.14. Consequently, our method outperforms all other methods.

Although our method achieves more balanced input sizes, model partitioning still constrained the training speed. Therefore, we also report results using model balancing (MB). With MB, the improvement is even greater, reducing GPU days from 42.2 to 29.0, a gain of 13.2, compared to a 9.9 improvement without MB (from 61.8 to 51.9 GPU days). This further underscores the importance of a holistic balance approach.

The Importance of Model Balance: In Table 5, we examine the impact of balanced model partitioning, particularly in the context of determining partition strategies for pipeline parallelism. For large language model (LLM) training, common partitioning methods include (1) parameter-based partitioning and (2) layer-based partitioning. Additionally, (3) profile-based methods such as DreamPipe Narayanan et al. (2019) estimate the computation time for each layer and use this information to partition the model effectively. Finally, (4) our search-based Balanced Model Partition method identifies the optimal partition strategy from a small set of partition candidates.

(1) Parameter-based and (2) layer-based methods split the model based on parameters or the number of layers, respectively. As shown in Table 5, these methods achieve the lowest variation in parameters (VAR(param)) and the number of layers (VAR(num.layer)) across devices, indicating balance in these metrics. However, due to the heterogeneous nature of vision and language models (VLMs), balancing parameters or layers does not equate to balanced computational loads. The variation in forward time (VAR(fwd.time)) for each stage remains high, at 93.6 and 20.1, respectively, leading to significant computational inefficiencies in the pipeline. The (3) profile-based method ensures the optimal VAR(fwd.time) with the lowest value of 6.5. However, this partitioning occurs before the vision model’s token sub-sampling operation, significantly increasing communication overhead by 16.6 compared to the baseline (1), thereby affecting training speed. Our proposed Balanced Model Partition (BMP) method searches within a high-quality partition space to find the optimal strategy. As shown in Table 5, our method achieves the best results, with 29.0 GPU days, outperforming the parameter-based method by 13.2 days. Notably, our method does not achieve low VAR(param) and VAR(num.layer), indicating that parameters and the number of layers are ineffective metrics for evaluating model balance in VLM scenarios.

The Importance of Memory Balance: We examine the significance of memory balance, with the results presented in Table 6. In the baseline model, the input sizes for both the vision and language components are not fixed, with vision token lengths ranging from 4K to 20K and language token lengths ranging from 1K to 16K. As a result, the memory demand on each GPU varies. Even with the most aggressive re-computation strategy, the remaining memory on an 80G A100 GPU can be as low as 7.3G in extreme cases. We achieved balance at both the data and model levels by implementing our proposed balanced dynamic mini-batch and model partition methods. This approach controls the computational load on each device and maintains relative balance, significantly improving training speed from 61.8 to 29.0 GPU days. However, due to inherent differences between vision and

Table 7: Results on different Model Size

Vision-Model	Language-Model	TP PP DP	Stages-Layer-Num (V+L)	Re-computation	GPU Days(speed up)
InternVL-6B	Llama3-8B	(1,4,8)	[16,17,20,24]	[8,7,10,24]	27.7 → 13.8(2.0x)
InternVL-6B	InternLM2-20B	(2,4,4)	[22,23,24,24]	[0,0,0,0]	61.8 → 21.3(2.9x)
InternVL-6B	Yi-34B	(4,4,2)	[28,29,24,24]	[3,2,0,0]	75.4 → 30.5(2.5x)
InternVL-6B	Llama3-70B	(4,8,2)	[22,23,13,14,14,14,13,12]	[11,12,8,5,3,2,0,0]	129 → 52.5(2.4x)
InternVL-6B	Qwen1.5-110B	(8,8,1)	[21,22,13,13,14,14,14,14]	[6,9,1,3,0,0,0,0]	243 → 75.2(3.2x)
EVA-CLIP-1B	InternLM2-20B	(2,4,4)	[43,16,15,14]	[0,0,0,0]	23.6 → 12.2(1.9x)
EVA-CLIP-4B	InternLM2-20B	(2,4,4)	[39,22,21,20]	[10,8,1,3]	38.1 → 17.0(2.2x)
EVA-CLIP-8B	InternLM2-20B	(2,4,4)	[17,18,23,22]	[5,5,8,10]	41.8 → 20.3(2.0x)
EVA-CLIP-18B	InternLM2-20B	(4,4,4)	[18,19,25,34]	[2,2,0,0]	63.6 → 33.8(1.9x)

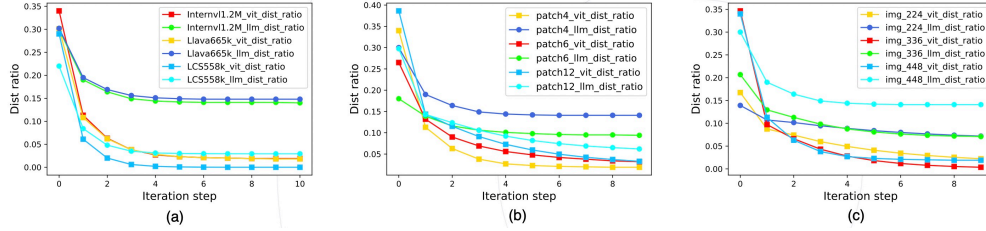


Figure 5: ISF convergence testing. We tested the convergence of ISF in various scenarios, including (a) different datasets, (b) different patch sizes, and (c) different image resolutions.

language models, their memory demands differ even under the same computational load, resulting in GPUs 3 and 4 having relatively low remaining memory. Our method further improves training speed by adaptive adjusting the re-computation strategy to utilize the remaining memory fully. As shown in the third row of Table 6, our method reduces GPU days from 29.0 to 21.3.

5.4 COMPONENT ANALYSIS

Convergence of ISF: We study the convergence performance of ISF, and the results are shown in Figure 5. On LLaVa-665K Liu et al. (2023a), we observed that the dist ratio in both the vision and language data was sufficiently low after just one iteration. After five iterations, the dist ratio stabilized significantly. In practice, we iterate ten times for stable results, which takes less than 1 minute. The computation cost is negligible compared to the overall runtime. We also tested our method on two additional datasets, InternVL-1.2M Chen et al. (2024) and LCS558K Liu et al. (2023b), and observed consistent convergence speeds. These findings demonstrate the effectiveness and generalizability of our method.

Generalization Capability: We studied the generalization capability of our method from multiple aspects: (1) Different Datasets: We conducted experiments on three different datasets. As shown in Table 3, we achieved consistently low dist ratios on LLaVa-665K, InternVL-1.2M, and LCS558K and significantly improved training speed. (2) Different Models: We tested various combinations of vision and language models. For vision models, in addition to InternVL-6B, we used the open-source EVA-CLIP models, ranging from 1B Sun et al. (2023a) to 18B Sun et al. (2023b). For language models, we employed Llama3-8B, 70B AI (2024), Yi-34B NousResearch (2023), and the large-scale Qwen1.5-110B Bai et al. (2023a). Table 7 shows our method greatly reduces GPU days for model training. Notably, we achieved a 3.2x speedup for the largest model, Qwen1.5-110B, demonstrating the advantages of our approach for large-scale VLM model training. (3) Different Tasks: Besides SFT tasks, we also tested pretraining tasks, as shown in Table 9. For models ranging from 6B to 20B, we trained both ViT and MLP components, and for larger models like 6B-34B and 6B-70B, we trained only the MLP component. We observed consistent improvements across all settings, especially for the largest model, where we reduced GPU days from 16.8 to 9.6. (4) Different Image Resolutions: We also test our method with different image resolutions input; from Table 10, it can be observed that our method also achieves a very satisfactory acceleration effect. (5) Different Model-series: We also validated our method using another popular open-source model, LLaVa-1.6,

Table 8: Results on Different Dynamic High-Resolution Setting

Model	Max-Patch-Num	AVE-BS	Max-Seq-Len		Dist Ratio		GPU Days
			VIT	LLM	VIT	LLM	
InternVL-6B-20B	1	7.6	9K	4K	0.06	0.05	28.6 \rightarrow 13.7
	4	4.6	9K	4K	0.02	0.14	61.8 \rightarrow 21.3
	6	2.7	14K	5K	0.019	0.136	147 \rightarrow 72
	12	1.9	14K	5K	0.03	0.12	209 \rightarrow 105

Table 9: Results on Pretrain Setting

Model	Dataset	Trainable Module	AVE-BS	Dist Ratio		GPU Days
				VIT	LLM	
InternVL-6B-20B	LCS-558K	ViT+MLP	5.8	0	0.03	9.9 \rightarrow 6.0
InternVL-6B-34B	LCS-558K	MLP	5.1	0	0.031	8.3 \rightarrow 4.9
InternVL-6B-70B	LCS-558K	MLP	5.2	0	0.029	16.8 \rightarrow 9.6

Table 10: Results on Different Resolutions

Resolution	AVE-BS	Dist Ratio		GPU Days
		VIT	LLM	
224	4.8	0.009	0.068	32.0 \rightarrow 20
336	3.3	0.005	0.07	62.0 \rightarrow 33
448	4.6	0.02	0.14	61.8 \rightarrow 21.3

Table 11: Results on Open-source Llava-1.6

Model	AVE-BS	Dist Ratio		GPU Days
		VIT	LLM	
Llava-1.6-7B	4.54	0.008	0.037	10.2 \rightarrow 7.7
Llava-1.6-13B	4.54	0.008	0.037	18 \rightarrow 13.3
Llava-1.6-34B	4.4	0.009	0.0041	42.7 \rightarrow 31.3

with the DeepSpeed backend, as shown in Table 11. These results highlight the effectiveness and robustness of our method across various datasets, models, and tasks.

6 CONCLUSION

In this work, we effectively addressed the issue of imbalanced computation loads in large-scale 3D parallel training of vision-language models by rebalancing across data, model, and memory dimensions. Experimental results demonstrate that our method can significantly reduce GPU days on many open-source models. The effectiveness and generalizability of our approach were also validated across various models, datasets, and hardware platforms. Our method can accelerate the development of this field by enabling more efficient training.

REFERENCES

- Meta AI. Introducing meta llama 3: The most capable openly available llm to date. <https://ai.meta.com/blog/meta-llama-3>, 2024.
- Jean-Baptiste Alayrac, Jeff Donahue, Pauline Luc, Antoine Miech, Iain Barr, Yana Hasson, Karel Lenc, Arthur Mensch, Katherine Millican, Malcolm Reynolds, Roman Ring, Eliza Rutherford, Serkan Cabi, Tengda Han, Zhitao Gong, Sina Samangooei, Marianne Monteiro, Jacob L Menick, Sebastian Borgeaud, Andy Brock, Aida Nematzadeh, Sahand Sharifzadeh, Mikołaj Bińkowski, Ricardo Barreira, Oriol Vinyals, Andrew Zisserman, and Karén Simonyan. Flamingo: a visual language model for few-shot learning. In S. Koyejo, S. Mohamed, A. Agarwal, D. Belgrave, K. Cho, and A. Oh (eds.), *Advances in Neural Information Processing Systems*, volume 35, pp. 23716–23736. Curran Associates, Inc., 2022. URL https://proceedings.neurips.cc/paper_files/paper/2022/file/960a172bc7fbf0177ccccbb411a7d800-Paper-Conference.pdf.
- Jinze Bai, Shuai Bai, Yunfei Chu, Zeyu Cui, Kai Dang, Xiaodong Deng, Yang Fan, Wenbin Ge, Yu Han, Fei Huang, Binyuan Hui, Luo Ji, Mei Li, Junyang Lin, Runji Lin, Dayiheng Liu, Gao Liu,

- Chengqiang Lu, Keming Lu, Jianxin Ma, Rui Men, Xingzhang Ren, Xuancheng Ren, Chuanqi Tan, Sinan Tan, Jianhong Tu, Peng Wang, Shijie Wang, Wei Wang, Shengguang Wu, Benfeng Xu, Jin Xu, An Yang, Hao Yang, Jian Yang, Shusheng Yang, Yang Yao, Bowen Yu, Hongyi Yuan, Zheng Yuan, Jianwei Zhang, Xingxuan Zhang, Yichang Zhang, Zhenru Zhang, Chang Zhou, Jingren Zhou, Xiaohuan Zhou, and Tianhang Zhu. Qwen technical report. *arXiv preprint arXiv:2309.16609*, 2023a.
- Jinze Bai, Shuai Bai, Shusheng Yang, Shijie Wang, Sinan Tan, Peng Wang, Junyang Lin, Chang Zhou, and Jingren Zhou. Qwen-vl: A versatile vision-language model for understanding, localization, text reading, and beyond. *arXiv preprint arXiv:2308.12966*, 2023b.
- Zhe Chen, Jiannan Wu, Wenhai Wang, Weijie Su, Guo Chen, Sen Xing, Muyan Zhong, Qinglong Zhang, Xizhou Zhu, Lewei Lu, Bin Li, Ping Luo, Tong Lu, Yu Qiao, and Jifeng Dai. Internvl: Scaling up vision foundation models and aligning for generic visual-linguistic tasks. *arXiv preprint arXiv:2312.14238*, 2023.
- Zhe Chen, Weiyun Wang, Hao Tian, Shenglong Ye, Zhangwei Gao, Erfei Cui, Wenwen Tong, Kongzhi Hu, Jiapeng Luo, Zheng Ma, et al. How far are we to gpt-4v? closing the gap to commercial multimodal models with open-source suites. *arXiv preprint arXiv:2404.16821*, 2024.
- Wenliang Dai, Junnan Li, Dongxu Li, Anthony Meng Huat Tiong, Junqi Zhao, Weisheng Wang, Boyang Li, Pascale Fung, and Steven Hoi. Instructblip: towards general-purpose vision-language models with instruction tuning. In *Proceedings of the 37th International Conference on Neural Information Processing Systems, NIPS '23*, Red Hook, NY, USA, 2024. Curran Associates Inc.
- Alexey Dosovitskiy, Lucas Beyer, Alexander Kolesnikov, Dirk Weissenborn, Xiaohua Zhai, Thomas Unterthiner, Mostafa Dehghani, Matthias Minderer, Georg Heigold, Sylvain Gelly, Jakob Uszkoreit, and Neil Houlsby. An image is worth 16x16 words: Transformers for image recognition at scale. *ICLR*, 2021.
- Chaoyou Fu, Peixian Chen, Yunhang Shen, Yulei Qin, Mengdan Zhang, Xu Lin, Zhenyu Qiu, Wei Lin, Jinrui Yang, Xiawu Zheng, et al. Mme: A comprehensive evaluation benchmark for multimodal large language models. *arXiv preprint arXiv:2306.13394*, 2023.
- Yanping Huang, Youlong Cheng, Ankur Bapna, Orhan Firat, Dehao Chen, Mia Chen, Hyoungho Joong Lee, Jiquan Ngiam, Quoc V Le, Yonghui Wu, et al. Gpipe: Efficient training of giant neural networks using pipeline parallelism. *Advances in neural information processing systems*, 32, 2019.
- Aniruddha Kembhavi, Mike Salvato, Eric Kolve, Minjoon Seo, Hannaneh Hajishirzi, and Ali Farhadi. A diagram is worth a dozen images. In *ECCV*, pp. 235–251, 2016.
- Junnan Li, Dongxu Li, Caiming Xiong, and Steven Hoi. Blip: Bootstrapping language-image pre-training for unified vision-language understanding and generation. In *ICML*, pp. 12888–12900, 2022.
- Junnan Li, Dongxu Li, Silvio Savarese, and Steven Hoi. Blip-2: Bootstrapping language-image pre-training with frozen image encoders and large language models. In *ICML*, pp. 19730–19742. PMLR, 2023.
- Mu Li, David G. Andersen, Jun Woo Park, Alexander J. Smola, Amr Ahmed, Vanja Josifovski, James Long, Eugene J. Shekita, and Bor-Yiing Su. Scaling distributed machine learning with the parameter server. In *11th USENIX Symposium on Operating Systems Design and Implementation (OSDI 14)*, pp. 583–598, Broomfield, CO, October 2014. USENIX Association. ISBN 978-1-931971-16-4. URL https://www.usenix.org/conference/osdi14/technical-sessions/presentation/li_mu.
- Haotian Liu, Chunyuan Li, Yuheng Li, and Yong Jae Lee. Improved baselines with visual instruction tuning, 2023a.
- Haotian Liu, Chunyuan Li, Qingyang Wu, and Yong Jae Lee. Visual instruction tuning. *NeurIPS*, 36, 2023b.

- Yuan Liu, Haodong Duan, Yuanhan Zhang, Bo Li, Songyang Zhang, Wangbo Zhao, Yike Yuan, Jiaqi Wang, Conghui He, Ziwei Liu, et al. Mmbench: Is your multi-modal model an all-around player? *arXiv preprint arXiv:2307.06281*, 2023c.
- Ahmed Masry, Xuan Long Do, Jia Qing Tan, Shafiq Joty, and Enamul Hoque. Chartqa: A benchmark for question answering about charts with visual and logical reasoning. In *ACL*, pp. 2263–2279, 2022.
- microsoft. Megatron-deepspeed. <https://github.com/microsoft/Megatron-DeepSpeed>, 2020.
- Deepak Narayanan, Aaron Harlap, Amar Phanishayee, Vivek Seshadri, Nikhil R Devanur, Gregory R Ganger, Phillip B Gibbons, and Matei Zaharia. Pipedream: generalized pipeline parallelism for dnn training. In *Proceedings of the 27th ACM symposium on operating systems principles*, pp. 1–15, 2019.
- NousResearch. Nous hermes 2 - yi-34b. <https://huggingface.co/NousResearch/Nous-Hermes-2-Yi-34B>, 2023.
- OpenAI. ChatGPT. <https://openai.com/blog/chatgpt/>, 2023a.
- OpenAI. Gpt-4 technical report, 2023b.
- Alec Radford, Jong Wook Kim, Chris Hallacy, Aditya Ramesh, Gabriel Goh, Sandhini Agarwal, Girish Sastry, Amanda Askell, Pamela Mishkin, Jack Clark, et al. Learning transferable visual models from natural language supervision. In *International conference on machine learning*, pp. 8748–8763. PMLR, 2021.
- Samyam Rajbhandari, Jeff Rasley, Olatunji Ruwase, and Yuxiong He. Zero: Memory optimizations toward training trillion parameter models. In *SC20: International Conference for High Performance Computing, Networking, Storage and Analysis*, pp. 1–16. IEEE, 2020.
- Machel Reid, Nikolay Savinov, Denis Teplyashin, Dmitry Lepikhin, Timothy Lillicrap, Jean-baptiste Alayrac, Radu Soricut, Angeliki Lazaridou, Orhan Firat, Julian Schrittwieser, et al. Gemini 1.5: Unlocking multimodal understanding across millions of tokens of context. *arXiv preprint arXiv:2403.05530*, 2024.
- Mohammad Shoeybi, Mostofa Patwary, Raul Puri, Patrick LeGresley, Jared Casper, and Bryan Catanzaro. Megatron-lm: Training multi-billion parameter language models using model parallelism. *arXiv preprint arXiv:1909.08053*, 2019.
- Quan Sun, Yuxin Fang, Ledell Wu, Xinlong Wang, and Yue Cao. Eva-clip: Improved training techniques for clip at scale. *arXiv preprint arXiv:2303.15389*, 2023a.
- Quan Sun, Jinsheng Wang, Qiyang Yu, Yufeng Cui, Fan Zhang, Xiaosong Zhang, and Xinlong Wang. Eva-clip-18b: Scaling clip to 18 billion parameters. *arXiv preprint arXiv:2402.04252*, 2023b.
- Zhenbo Sun, Huanqi Cao, Yuanwei Wang, Guanyu Feng, Shengqi Chen, Haojie Wang, and Wenguang Chen. Adapipe: Optimizing pipeline parallelism with adaptive recomputation and partitioning. In *Proceedings of the 29th ACM International Conference on Architectural Support for Programming Languages and Operating Systems, Volume 3*, pp. 86–100, 2024.
- Gemini Team, Rohan Anil, Sebastian Borgeaud, Yonghui Wu, Jean-Baptiste Alayrac, Jiahui Yu, Radu Soricut, Johan Schalkwyk, Andrew M Dai, Anja Hauth, et al. Gemini: a family of highly capable multimodal models. *arXiv preprint arXiv:2312.11805*, 2023a.
- Gemini Team, Rohan Anil, Sebastian Borgeaud, Yonghui Wu, Jean-Baptiste Alayrac, Jiahui Yu, Radu Soricut, Johan Schalkwyk, Andrew M Dai, Anja Hauth, et al. Gemini: a family of highly capable multimodal models. *arXiv preprint arXiv:2312.11805*, 2023b.
- Hugo Touvron, Thibaut Lavril, Gautier Izacard, Xavier Martinet, Marie-Anne Lachaux, Timothée Lacroix, Baptiste Rozière, Naman Goyal, Eric Hambro, Faisal Azhar, et al. Llama: Open and efficient foundation language models. *arXiv preprint arXiv:2302.13971*, 2023a.

Hugo Touvron, Louis Martin, Kevin Stone, Peter Albert, Amjad Almahairi, Yasmine Babaei, Nikolay Bashlykov, Soumya Batra, Prajjwal Bhargava, Shruti Bhosale, et al. Llama 2: Open foundation and fine-tuned chat models. *arXiv preprint arXiv:2307.09288*, 2023b.

Weihao Yu, Zhengyuan Yang, Linjie Li, Jianfeng Wang, Kevin Lin, Zicheng Liu, Xinchao Wang, and Lijuan Wang. Mm-vet: Evaluating large multimodal models for integrated capabilities. *arXiv preprint arXiv:2308.02490*, 2023.